Ozonolysis of Geraniol-trans, 6-Methyl-5-hepten-2-one, and 6-Hydroxy-4-methyl-4-hexenal: Kinetics and Mechanisms

Tadeu Leonardo,* Edilson Clemente da Silva, and Graciela Arbilla

Departamento de Físico-Química, Universidade Federal do Rio de Janeiro, Instituto de Química, CT Bloco A sala 408, Ilha do Fundão, Rio de Janeiro, Brasil

Received: October 29, 2007; Revised Manuscript Received: April 3, 2008

A combined density functional theory and transition-state theory study of the mechanisms and reaction coefficients of gas-phase ozonolysis of geraniol-trans, 6-methyl-5-hepten-2-one, and 6-hydroxy-4-methyl-4-hexenal is presented. The geometries, energies, and harmonic vibrational frequencies of each stationary point were determined by B3LYP/6-31(d,p), MPW1K/cc-pVDZ, and BH&HLYP/cc-pVDZ methods. According to the calculations, the ozone 6-methyl-5-hepten-2-one reaction is faster than the ozone 6-hydroxy-4-methyl-4-hexenal reaction, but both are slower than the ozone geraniol-trans reaction. By using the BH&HLYP/cc-pVDZ data, a global rate coefficient of 5.9×10^{-16} cm^3 molecule^{-1} s^{-1} was calculated, corresponding to the sum of geraniol-trans, 6-methyl-5-hepten-2-one, and 6-hydroxy-4-methyl-4-hexenal reactions with the ozone. These results are in good agreement with the experimental studies.

I. Introduction

Biogenic emissions of volatile organic compounds (VOCs) play a major role in the atmospheric chemistry of rural and remote areas, exceeding by orders of magnitude those of the anthropogenic origin, with vegetation as the most important natural source of these compounds.[1] Terpenoids represent the most abundant VOCs emitted by plants, with an estimated global emission rate[2] on the order of 10^{14} g yr^{-1} and constitute an extensive class of compounds, the most volatile of which being mono-(C_{10}) and sesquiterpenoids (C_{15}) that represent the major components[3] of essential oils. Monoterpenoids may have acyclic, monocyclic, and bicyclic structures and occur in nature as hydrocarbons, alcohols, ketones, aldehydes, ethers, and other.[3]

In this work, the acyclic monoterpenoid 2,6-dimethyl-2,6-octadien-8-ol (geraniol-trans, see Structure1) is studied. This compound is found in the essential oils of plants in Brazil,[4] as oil of rose, palma rosa, and citronella oil (Java type) and is probably present in the air, through emissions from these plants. It is, therefore, important for the understanding of the chemical phenomena occurring in atmospheres over rural regions of Brazil, where the presence of this type of vegetation occurs. This compound is also a significant component of indoor cleaner emissions. The primary atmospheric degradation pathways of geraniol-trans[5] are reactions with OH and NO_3 radicals and O_3. Although the atmospheric residence time of geraniol-trans is mainly determined by reactions with OH and NO_3 radicals, the ozonolysis is also important. There exists increasing evidence that the ozonolysis process contributes to OH radical formation.[6] Recent atmospheric measurements indicate that ozonolysis of terpenes likely provides a missing OH reactivity observed over forested areas.[6]

The primary products are 6-methyl-5-hepten-2-one and 6-hydroxy-4-methyl-4-hexenal, which are also reactive species.

Reactions of O_3 with geraniol-trans, 6-methyl-5-hepten-2-one, and 6-hydroxy-4-methyl-4-hexenal lead to formation of potential precursors of secondary organic aerosols (SOA). SOA formations from biogenic sources are believed to have profound impacts on human health and climate.[5] Hence, it is of vital importance to quantitatively understand the roles of ozonolysis of geraniol-trans, 6-methyl-5-hepten-2-one, and 6-hydroxy-4-methyl-4-hexenal in OH and SOA formation in the troposphere.

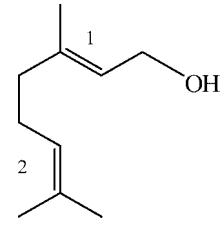

The O_3 reactions with geraniol-trans, 6-methyl-5-hepten-2-one, and 6-hydroxy-4-methyl-4-hexenal follow the Criegee mechanism of alkene ozonolysis.[6] The initial stage of this reaction involves the 1,3-dipolar addition of O_3 to the C=C bond, which gives rise to the production of a primary ozonide (molozonide) which is highly unstable and cleaves via a cycloreversion through two different routes.[7] Recently, the structures of the gas-phase ozonides of β-pinene and sabinene were successfully isolated and described,[8] thus demonstrating, for the first time, the formation of these intermediate compounds in the ozonolysis of the gas phase of monoterpenoids. The excited primary ozonide subsequently undergoes decomposition to yield chemically activated carbonyl oxides or Criegee intermediates (CIs) and aldehydes and ketones. A large fraction of the carbonyl oxides has ample internal energy and is subjected to prompt unimolecular reactions or collisional stabilization. There are two reaction pathways for the carbonyl oxide, ring closure to dioxirane or H migration to a hydroperoxide intermediate. The hydroperoxide subsequently undergoes isomerization or decomposition, which leads to formation of OH, carbonyls, CO_2, and a variety of other products, some of which are potential SOA precursors. Thermally stabilized CIs may undergo bimolecular reactions with atmospheric H_2O, SO_2, HCHO, and so forth.[6]

* Corresponding author. Fax: (55) 21 2562−7265. Tel: (55) 21 2562−7755. E-mail:graciela@iq.ufrj.br.

10.1021/jp8027534 CCC: $40.75
Published on Web 06/28/2008

SCHEME 1

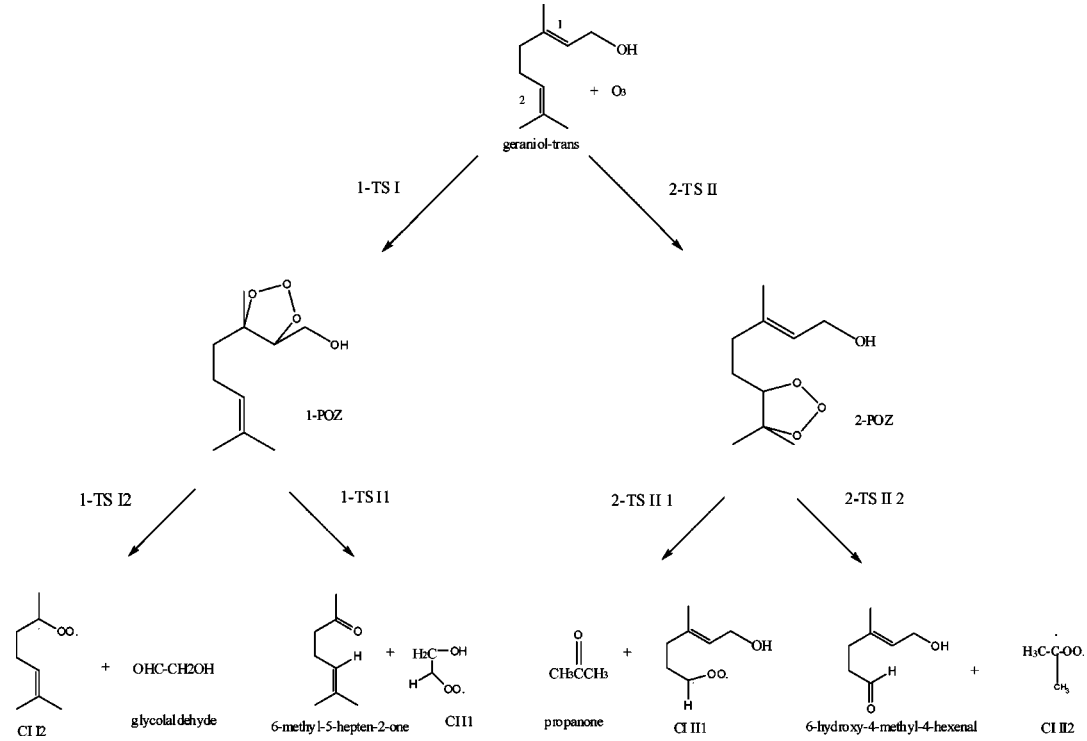

SCHEME 2

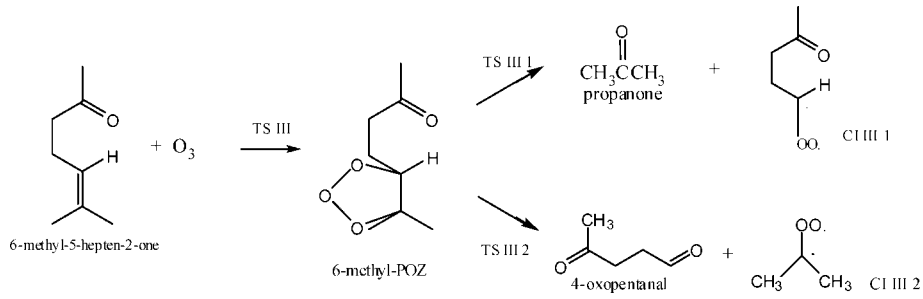

SCHEME 3

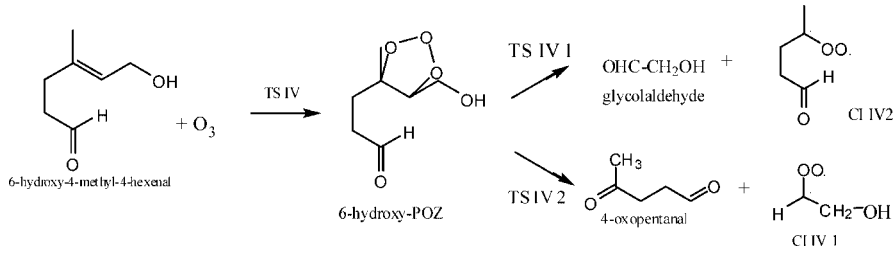

Schemes 1, 2, and 3 illustrate the mechanism of O_3 reactions with geraniol-trans, 6-methyl-5-hepten-2-one, and 6-hydroxy-4-methyl-4-hexenal, respectively.

A number of laboratory studies have been performed to investigate the reaction of O_3 with geraniol-trans, 6-methyl-5-hepten-2-one, and 6-hydroxy-4-methyl-4-hexenal. Ozone reacts with geraniol-trans by addition to the carbon−carbon double bond (sites 1 and 2, Structure 1). Several kinetic studies measured rate constants for cycloaddition of O_3 to geraniol-trans and 6-methyl-5-hepten-2-one.[5,9,10] The reported rates are in the range of $(4.0-9.3) \times 10^{-16}$ cm^3 molecule^{-1} s^{-1} for geraniol-trans[5,9,10] and 390.0×10^{-18} cm^3 molecule^{-1} s^{-1} for 6-methyl-5-hepten-2-one.[9] The reaction products of ozonolysis of geraniol-trans, 6-methyl-5-hepten-2-one, and 6-hydroxy-4-methyl-4-hexenal have been identified. Propanone, glycoaldehyde, 4-oxo-pentanal, glyoxal, and methylglyoxal were identified as the most abundant stable products of geraniol-trans, 6-methyl-5-hepten-2-one, and 6-hydroxy-4-methyl-4-hexenal ozonolysis.[5]

Despite the enormous interest in the reactions of O_3 with geraniol-trans, 6-methyl-5-hepten-2-one, and 6-hydroxy-4-methyl-4-hexenal, there still exist considerable uncertainties about the reaction mechanisms and product yields. Except for the initial step, there are currently no experimental or theoretical kinetic data on the subsequent reactions. Experimental detection of the intermediate species is extremely difficult because of their short lifetimes. Several efforts to elucidate the reaction mechanism are hindered because of the uncertain fate of the reactive intermediates. Although several theoretical studies have investigated ozonolysis of other alkenes and terpenes such as α- and

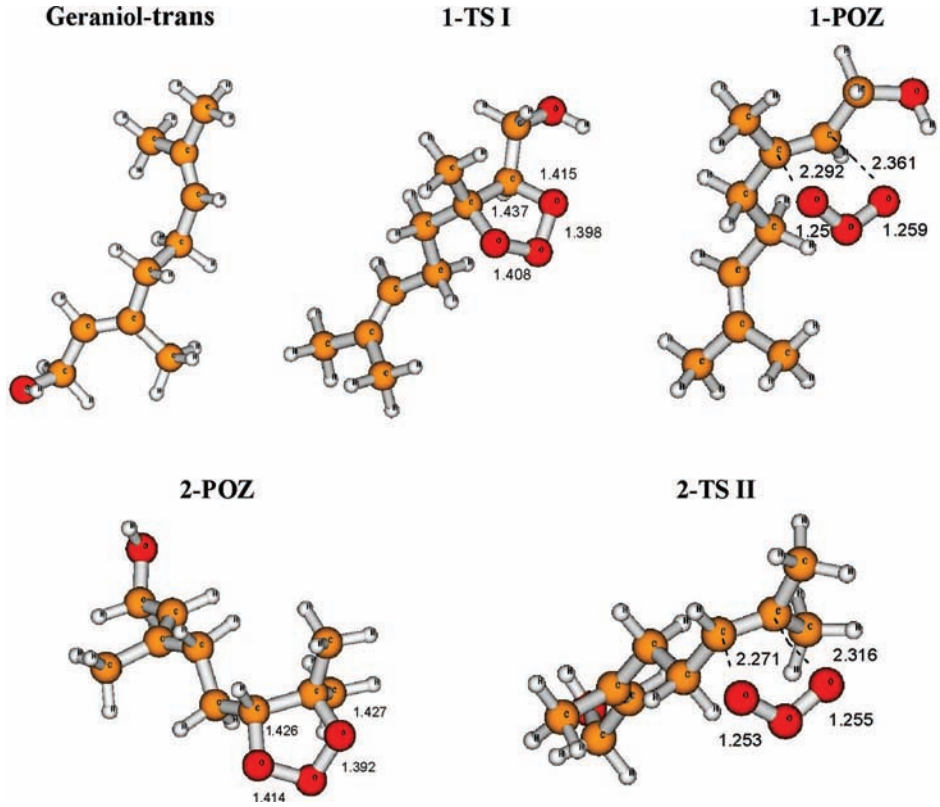

Figure 1. Optimized geometries of geraniol-trans, primary ozonides, and the transition states for the primary ozonide formation calculated at the BH&HLYP/cc-pVDZ level of theory (bond lengths in angstroms).

TABLE 1: Gibbs Free Energy of Activation for the Intermediate Pathways of Geraniol-trans Ozonolysis Reactions at 298 K (kcal mol^{-1})

pathway	B3LYP/6-31 (d,p)	MPW1K/cc-pVDZ	BH&HLYP/cc-pVDZ
I	7.1	8.8	9.8
II	8.7	10.9	12.2
I 1	16.2	27.1	28.6
I 2	15.4	26.0	27.5
II 1	17.8	28.4	30.2
II 2	16.3	26.9	28.6

TABLE 2: Calculated TST Rate Coefficients for the Intermediate Pathways of Geraniol-trans Ozonolysis Reaction at 298 K at the BH&HLYP/cc-pVDZ Level of Theory[a]

pathway	k
I	5.8×10^{-16}
II	1.1×10^{-17}
I 1	8.3×10^{-30}
I 2	6.5×10^{-29}
II 1	7.1×10^{-31}
II 2	9.9×10^{-30}

[a] Units of s^{-1} and cm^3 molecule^{-1} s^{-1} for unimolecular and bimolecular coefficients, respectively.

β-pinenes,[6] no report of the ozonolysis of geraniol-trans, 6-methyl-5-hepten-2-one, and 6-hydroxy-4-methyl-4-hexenal is available.

In this study, a work to demonstrate the theoretical methods applicable to large hydrocarbon molecules such as geraniol-trans, 6-methyl-5-hepten-2-one, and 6-hydroxy-4-methyl-4-hexenal and to elucidate their reaction mechanisms with ozone is presented. The study includes formation of the primary ozonides and cleavage of the primary ozonides to form carbonyl oxides, aldehydes, and ketones. Density functional theory (DFT) methods were employed to obtain the geometries, energies, and harmonic vibrational frequencies of each stationary point. On the basis of the quantum-chemical results, the bimolecular and unimolecular rate constants at the high-pressure limit were calculated by following the thermodynamic interpretation of transition state theory (TST) equation. The present theoretical work is compared with available experimental measurements of the rate constants and stable products.

II. Theoretical Method

A. Quantum-Chemical Calculations. The ozonolysis of geraniol-trans (2,6-dimethyl-2,6-octadien-8-ol), 6-methyl-5-hepten-2-one, and 6-hydroxy-4-methyl-4-hexenal involves a large number of reactions and species. It is important to choose suitable methods of quantum chemistry to investigate these reactions. Cremer et al.[11] and Li et al.[12] checked various methods and found that the density functional method can provide a reasonable description of ozonolysis reactions. A recent work by Zhao and Truhlar[13] has tested the performance of 44 density functionals in the description of unbonded interactions. They analyzed hydrogen-bond type interactions, charge transfer, dipole interactions, and van der Waals interactions. The functionals were classified according to the calculation accuracy in reproducing each of these interactions over a ranking ordered in accordance with the performance of each functional.

In this study, the theoretical computations were performed using Gaussian 98 software package[14] in order to evaluate the structures and energies of the reactants, intermediates, transition states, and products involved in the reaction. The geometries, energies, and harmonic vibrational frequencies of each stationary point considered in this study were determined initially by using the B3LYP functional and the 6-31G(d,p) basis set. Each reported minimum has all real frequencies, and each reported

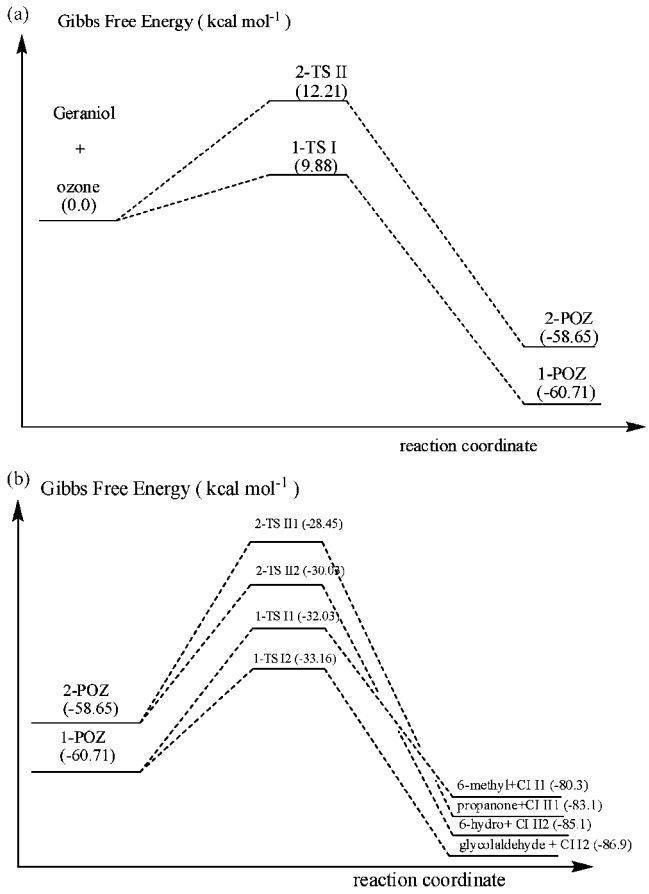

Figure 2. Gibbs free-energy profile for (a) the geraniol-trans ozonolysis and (b) the cleavage of primary ozonides.

transition structure has one imaginary frequency. The transition states were searched by using constrained geometry optimization at fixed C−O bond lengths by using B3LYP/3-21G(d). First considered were the equilibrium structures of the primary ozonides as the initial guess for the transition states. The two C−O bond lengths were then successfully increased by a fixed increment relative to the equilibrium C−O bond length of the primary ozonide. Once a transition state was located, the geometry was optimized at the B3LYP/6-31G(d,p) level of theory.

Because the B3LYP method tends to underestimate hydrogen-shift reaction barriers and may provide unreliable thermochemical predictions,[6] the geometry of each stationary point was recomputed according to the MPW1K[15] DFT and cc-pVDZ basis set. MPW1K is a DFT method suggested by Truhlar and coworkers and has been developed on the basis of the MPW1PW91[16] functional (Barone and Adamo's Becke-style one-parameter functional using the modified Perdew−Wang exchange function and Perdew−Wang 91 correlation functional). MPW1K is competitive in predicting energies and geometries of compounds, especially in predicting the classical barrier height and standard reaction enthalpies.[17,18] The geometry of each stationary point was then recomputed at the BH&HLYP[19]/cc-pVDZ level of theory. The nature of each stationary point was determined by calculating harmonic vibrational frequencies at the MPW1K/cc-pVDZ and BH&HLYP/cc-pVDZ levels of theory. Each minimum was confirmed to have only real frequencies and each transition structure to have only one imaginary frequency. The minima associated with each transition structure were connected with intrinsic reaction coordinate (IRC) calculations. The calculated absolute energies, harmonic frequencies, and zero-point energies of all the molecules considered in this work are given in the Supporting Information.

B. Kinetic Calculations. It was assumed that the unimolecular reaction pathways of the primary ozonide and carbonyl oxide are irreversible. Usually, one can safely ignore recombinations in a gaseous environment as the chances of the products encountering each other again before collisional deactivation is miniscule. The bimolecular and unimolecular rate coefficients at the high-pressure limit were calculated by following the thermodynamic interpretation of the TST equation:[20]

$$k = (k_b T/\hbar) \exp(-\Delta G^*/RT)$$

where ΔG^* is the free energy of activation, k_b is the Boltzman constant, and $\hbar$ is the Planck constant, considering $T = 298.15$ K and the standard state of 1 mol L^{-1}.

III. Results and Discussion

The ozonolysis of geraniol-trans, 6-methyl-5-hepten-2-one, and 6-hydroxy-4-methyl-4-hexenal may be considered to occur in three steps: formation of primary ozonides, cleavage of primary ozonides to produce carbonyl oxides and products, and the competing pathways of the carbonyl oxides associated with the formation of the glyoxal and methylglyoxal. In this paper, only the two initial steps will be discussed; the third step will be shown in another paper.

A.1. Formation of Primary Ozonides for Geraniol-trans Ozonolysis. As illustrated in Scheme 1, the initial step of ozonolysis of geraniol-trans occurs via the concerted addition of ozone to the double bonds 1 and 2, each forming a primary ozonide (**1-POZ** and **2-POZ**). The lowest energy geometry of the primary ozonides was found to resemble the O-envelope conformation as decribled by Cremer and Pople,[21] similar to the analogous O_3-α-pinene and O_3-β-pinene reactions in previous ab initio studies.[6] Harmonic frequency calculations of the optimized POZ structures indicated that the optimized geometries represented minima on the potential energy surface.

Two transition states, **1-TS I** and **2-TS II**, were identified associated with the formation of the primary ozonides from geraniol-trans, **1-POZ** and **2-POZ**, respectively. Harmonic frequency calculations were performed and for each transition state, only one imaginary vibrational frequency was found, which confirms the first-order saddle point configuration. Additional calculations using the IRC method were performed for the transition state, showing that each transition state effectively connected the reactants (ozone and geraniol-trans) and the products (**1-POZ** and **2-POZ**). The optimized geometries of geraniol-trans, **1-POZ**, **1-TS I**, **2-POZ**, and **2-TS II**, at the BH&HLYP/cc-pVDZ level of theory, are given in Figure 1. Similar to that of **POZs,** the structures of **1-TS I** and **2-TS II** were observed to also resemble the O-envelope conformation. As shown in Figure 1, the C−O distances of the transition states are between 2.27 and 2.36 Å, 0.84−0.94 Å longer than those of the corresponding primary ozonides at the BH&HLYP/cc-pVDZ level of theory.

The free energies of activation for the reaction pathways shown in Scheme 1 are summarized in Table 1 for the geraniol-trans reaction.

The free energies of the activation are 12.21 kcal mol^{-1} for **2-TSII** and 9.88 kcal mol^{-1} for **1-TSI** at the BH&HLYP/cc-pVDZ level of theory. The results herein presented are consistent with theoretical studies of ozonolysis of α-pinene and β-pinene.[6] The rate coefficients for O_3 addition to geraniol-trans were

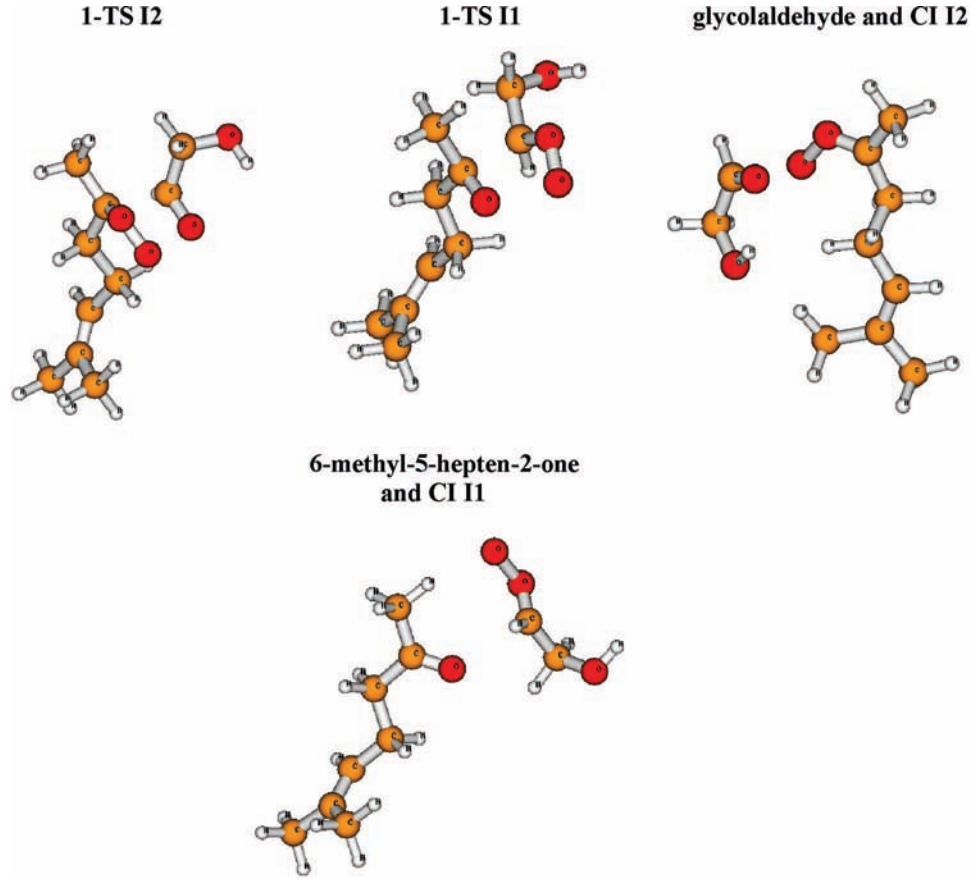

Figure 3. Optimized geometries of 1-TS I2, 1-TS I1, glycolaldehyde, 6-methyl-5-hepten-2-one, CI I2, and CI I1, associated with cleavage of the primary ozonide 1-POZ at the BH&HLYP/cc-pVDZ level of theory.

calculated by using the TST equation and the free energies of activation obtained at the BH&HLYP/cc-pVDZ level (see Table 2). For pathways I and II, the values 5.8×10^{-16} and 1.1×10^{-17} cm^3 molecule^{-1} s^{-1} at 298 K, respectively, were obtained. For the geraniol-trans reaction, the most recent experimental measurements suggest a rate coefficient in the range of $(4.0-9.3) \times 10^{-16}$ cm^3 molecule^{-1} s^{-1} at 298 K.[5,9]

For O_3 cycloaddition, the free energies of activation predicted at the MPW1Kcc-pVDZ and BH&HLYP/cc-pVDZ levels are comparable but higher than those obtained at the B3LYP/631-(d,p) level. At the BH&HLYP/cc-pVDZ level of theory, the two primary ozonides are 58.65 and 60.71 kcal mol^{-1} more stable than the separate O_3 and geraniol-trans, respectively. The Gibbs free-energy profile for the geraniol-trans ozonolysis calculated by using BH&HLYP/cc-pVDZ is depicted in Figure 2a,b.

A.2. Cleavage of Primary Ozonides and Formation of Carbonyl Oxides for Geraniol-trans Ozonolysis. A previous ab initio study of α-pinene and β-pinene[6] suggested only concerted pathways for the decomposition of the primary ozonides. The concerted unimolecular reactions of **1-POZ** and **2-POZ** occur via the simultaneous cleavage of the C−C bond and one of the O−O bonds in the five-membered ring.

For **1-POZ**, cleavage of the highly strained bicyclic ring structure forms two possible distinct carbonyl oxides (CIs), **CI I1**and **CI I2**, and the stable **glycolaldehyde** and **6-methyl-5-hepten-2-one**, as shown in Scheme 1. The optimized geometries of carbonyl oxides and products are shown in Figure 3. The CCOO group exhibits a nearly planar configuration in both CIs, with the dihedral angles of 0.2 degree for **CI I1** and 2 degrees for **CI I2**. For **CI I1**, the OO unit is in the syn position relative to the OH group, while for **CI I2** the OO unit is in the antiposition relative to the methyl group.

Cleavage of **2-POZ** occurs via two plausible pathways to form stable **propanone** and **6-hydroxy-4-methyl-4-hexenal** with the CIs **CI II1** and **CI II2** as shown in Scheme 1. **Propanone**, **glycolaldehyde**, **glyoxal**, **methylglyoxal**, and **4-oxopentanal** have been identified as the final products from geraniol-trans ozonolysis[5]. There is evidence that **propanone**, **glycolaldehyde**, **glyoxal**, and **4-oxopentanal** are also produced in the reactions of 6-hydroxy-4-methyl-4-hexenal and 6-methyl-5-hepten-2-one with ozone.[5] **4-Oxopentanal** has been identified as a major final product from geraniol-trans ozonolysis.[5] The optimized geometries of carbonyl oxides and products are shown in Figure 4. The CCOO group exhibits a nearly planar configuration in both CIs, with the dihedral angles of 0.1° for **CI II1** and 2° for **CI II2**.

The transition states **1-TS I1**, **1-TS I2**, **2-TS II1**, and **2-TS II2** were determined for the decomposition of **1-POZ** and **2-POZ** ozonides by using the B3LYP, MPW1K, and BH&HLYP levels of theory. Cleavage of the envelope conformations of the primary ozonides occurs via a strongly bent envelope-looking transition state. As depicted in Figures 3 and 4, the lengths for breaking the C−C and O−O bonds in the transition states are in the ranges of 1.40 and 1.29, respectively. The free energy of activation for cleavage of **1-POZ** and **2-POZ** obtained at B3LYP/6-31(d,p) are 30−40% smaller than those computed in the MPW1K/cc-pVDZ and BH&HLYP/cc-pVDZ methods. In Table 3, the calculated rate coefficients for the pathways of Scheme 1 are shown. The free energy of activation obtained at the MPW1K/cc-pVDZ and BH&HLYP/cc-pVDZ levels are rather similar, with a difference of 1.1 kcal mol^{-1} between the

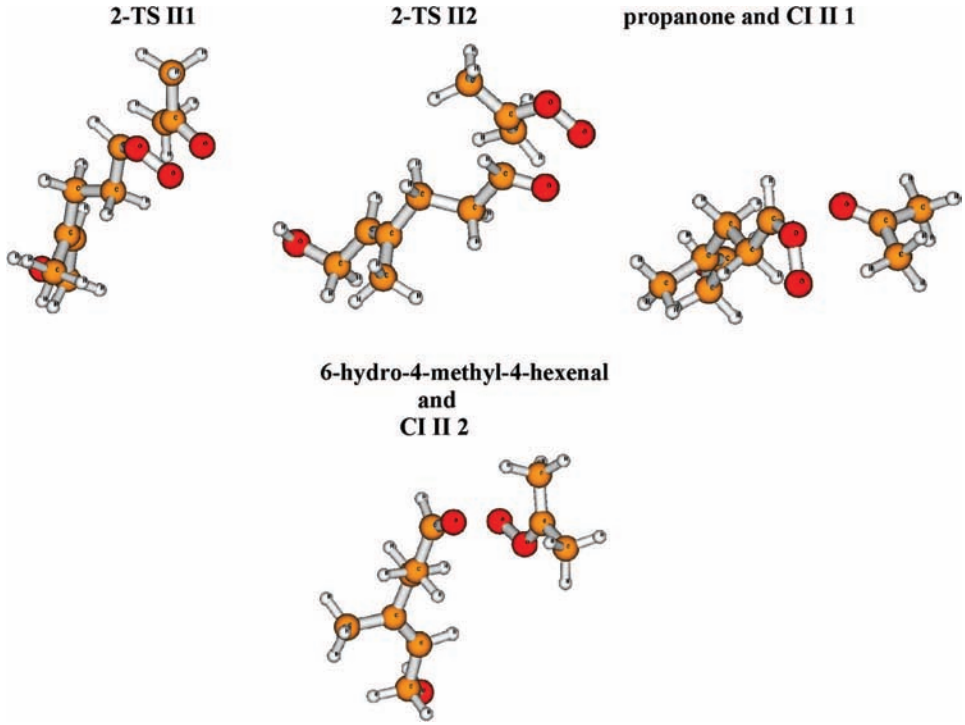

Figure 4. Optimized geometries of 2-TS II1, 2-TS II2, propanone, 6-hydro-4-methyl-4-hexenal, CI II 1, and CI II 2 associated with cleavage of the primary ozonide 2-POZ at the BH&HLYP/cc-pVDZ level of theory.

TABLE 3: Gibbs Free Energy of Activation for the Intermediate Pathways of 6-Methyl-5-hepten-2-one and 6-Hydroxy-4-methyl-4-hexenal Ozonolysis Reactions at 298 K (kcal mol^{-1})

pathway	MPW1K/cc-pVDZ	BH&HLYP/cc-pVDZ
III	11.2	12.5
III 1	28.9	30.5
III 2	28.0	29.4
IV	12.7	13.5
IV 1	25.0	29.7
IV 2	28.0	26.6

two methods. At the BH&HLYP/cc-pVDZ level, **1-TS I2** pathway possesses a lower free energy of activation, leading to **glycolaldehyde** and **CI I 2** which are 1.1 kcal more stable than **6-methyl-5-hepten-2-one** and **CI I1**. For **2-POZ** decomposition, the pathway leading to **6-hydro-4-methyl-4-hexenal** and **CI II 2** is more favorable, with a free energy of activation 1.6 kcal mol^{-1} lower than that of the propanone and **CI II 1** pathway.

B.1. Formation of Primary Ozonides for 6-Methyl-5-hepten-2-one and 6-Hydroxy-4-methyl-4-hexenal Ozonolysis. The initial step of ozonolysis of 6-methyl-5-hepten-2-one and 6-hydroxy-4-methyl-4-hexenal occurs via the concerted addition of ozone to the double bond of 6-methyl-5-hepten-2-one and 6-hydroxy-4-methyl-4-hexenal, each forming a primary ozonide (**6-methyl-POZ** and **6-hydroxy-POZ**). The lowest energy geometry of the primary ozonides was found to resemble the O-envelope conformation as described by Cremer and Pople,[21] similar to the analogous O_3-α-pinene and O_3-β-pinene reactions in previous ab initio studies.[6] Harmonic frequency calculations of the optimized POZ structures indicated that the optimized geometries represented minima on the potential energy surface.

Two transition states, **TS III** and **TS IV**, were identified and associated with the formation of the primary ozonides from 6-methyl-5-hepten-2-one and 6-hydroxy-4-methyl-4-hexenal, respectively. Harmonic frequency calculations were performed and for each transition state, only one imaginary vibrational frequency was used, which confirms the first-order saddle point configuration. Additional calculations using the IRC method were performed by starting from the transition state, thus showing that each TS effectively connected the reactants (**ozone**, **6-methyl-5-hepten-2-one**, and **6-hydroxy-4-methyl-4-hexenal**) and the products (**6-methyl-POZ** and **6-hydroxy-POZ**). The optimized geometries of **6-methyl-5-hepten-2-one**, **6-hydroxy-4-methyl-4-hexenal**, **6-methyl-POZ**, **TS III**, **6-hydroxy-POZ**, and **TS IV**, at the BH&HLYP/cc-pVDZ level of theory, are shown in Figure 5. Similar to **POZs**, the structures of **TS III** and **TS IV** were also found to resemble the O-envelope conformation. As shown in Figure 5, the C−O distances of the transition states are between 2.21 and 2.43 Å, 0.78−1.02 Å longer than those of the corresponding primary ozonides at the BH&HLYP/cc-pVDZ level of theory.

The free energies of activation for the reaction pathways shown in Schemes 2 and 3 are summarized in Table 3 for the 6-methyl-5-hepten-2-one and 6-hydroxy-4-methyl-4-hexenal reactions, respectively.

The free energies of activation are 12.5 kcal mol^{-1} for TS III and 13.5 kcal mol^{-1} for TS IV at the BH&HLYP/cc-pVDZ level of theory. The rate coefficients for O_3 addition to 6-methyl-5-hepten-2-one and 6-hydroxy-4-methyl-4-hexenal were calculated by using the TST expression and the free energy of activation obtained at the BH&HLYP/cc-pVDZ level. By using the optimized geometries and free energies of activation, the TST rate coefficients of 6.6×10^{-18} cm^3 molecule^{-1} s^{-1} for 6-methyl-5-hepten-2-one and 1.2×10^{-18} cm^3 molecule^{-1} s^{-1} for 6-hydroxy-4-methyl-4-hexenal, at 298 K, were determined. For the 6-methyl-5-hepten-2-one reaction, the most recent measurements suggests a rate coefficient[9] in the range of 394×10^{-18} cm^3 molecule^{-1} s^{-1} at 298 K. For O_3 cycloaddition, the free energy of activation predicted at MPW1Kcc-pVDZ and BH&HLYP/cc-pVDZ are comparable. At the BH&HLYP/cc-pVDZ level of theory, the two primary ozonides are 58.5 and

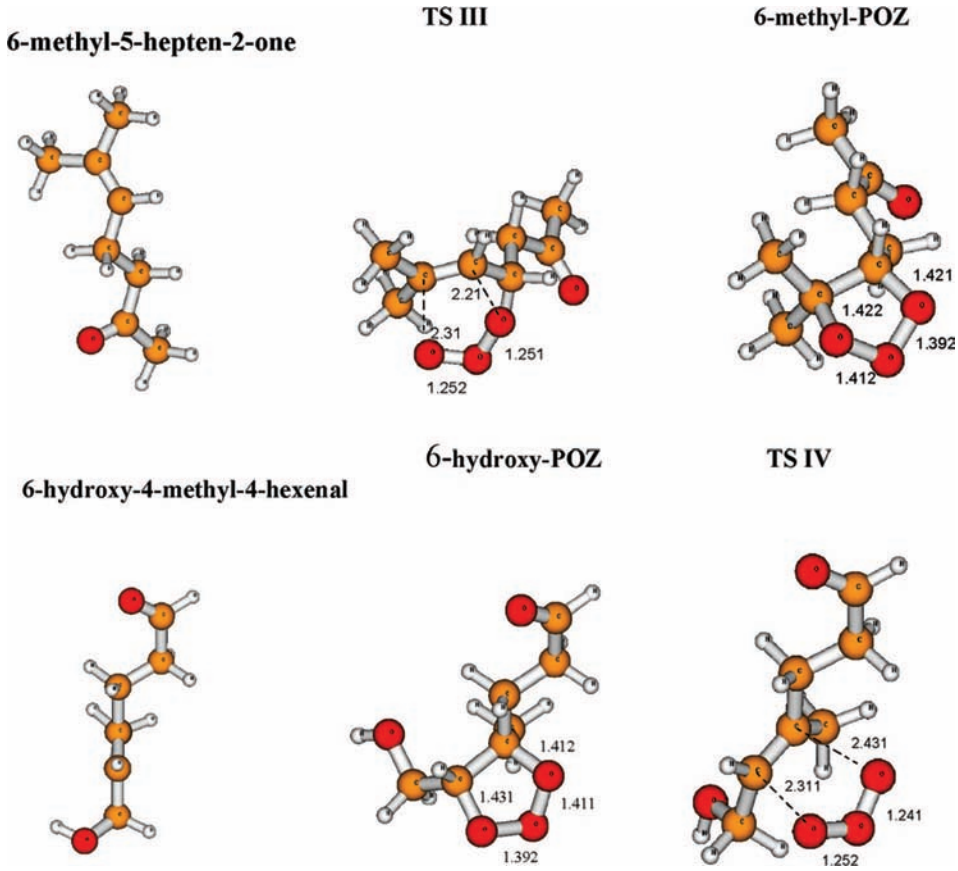

Figure 5. Optimized geometries of 6-methyl-5-hepten-2-one, 6-hydroxy-4-metil-4-hexenal, 6-methyl-POZ, 6-hydroxy-POZ, and the transition states for the primary ozonide formation TS III and TS IV calculated at the BH&HLYP/cc-pVDZ level of theory (bond lengths in angstroms).

60.5 kcal mol^{-1} more stable than the separate O_3 6-methyl-5-hepten-2-one and 6-hydroxy-4-methyl-4-hexenal, respectively.

B.2. Cleavage of Primary Ozonides and Formation of Carbonyl Oxides for 6-Methyl-5-hepten-2-one and 6-Hydroxy-4-methyl-4-hexenal Ozonolysis. The concerted unimolecular reactions of 6-methyl-POZ and 6-hydroxy-POZ occur via the simultaneous cleavage of the C−C bond and one of the O−O bonds in the five-membered ring.

For 6-methyl-POZ, cleavage of the highly strained bicyclic ring structure forms two possible distinct carbonyl oxides (CIs), CI III 1 and CI III 2, and the stable propanone and 4-oxo-pentanal as shown in Scheme 2. The optimized geometries of TS, carbonyl oxides, and products are depicted in Figure 6. The CCOO group exhibits a nearly planar configuration in both CIs, with the dihedral angles of 0.2° for CI III 1 and 1° for CI III 2. For CI III 1, the OO unit is in the antiposition relative to the CH, whereas for CI III 2, the OO unit is in the syn position relative to the methyl group.

Cleavage of 6-hydroxy-POZ occurs via two plausible pathways to form stable glycolaldehyde and 4-oxo-pentanal with the Criegee intermediate CI IV 1 and CI IV 2, as shown in Scheme 3. The optimized geometries of TS, carbonyl oxides, and products are illustrated in Figure 7. The CCOO group exhibits a nearly planar configuration in both CIs, with the dihedral angles of 1.0° for CI IV1 and 1.5° for CI IV2.

The transition states TSIII 1, TSIII 2, TS IV 1, and TS IV 2 were located for the decomposition of 6-methyl-POZ and 6-hydroxy-POZ ozonides at the B3LYP, MPW1K, and BH&HLYP levels of theory. Cleavage of the envelope conformations of the primary ozonides occurs via a strongly bent envelope-looking transition state. As depicted in Figure 2, the lengths for breaking the C−C and O−O bonds in the transition states are in the ranges of 1.37 and 1.25 for 6-methyl-POZ and 1.33 and 1.22 for 6-hydroxy-POZ, respectively. The Gibbs free-energy profile for the 6-methyl-5-hepten-2-one and 6-hydroxy-4-methyl-4-hexenal ozonolysis calculated by using BH&HLYP/cc-pVDZ are shown in Figures 8a−d.

At the BH&HLYP/cc-pVDZ level, the free energy of activation for 6-methyl-POZ is 30.56 kcal mol^{-1} for propanone and CI III 1 pathway and 29.46 kcal mol^{-1} for 4-oxo-pentanal and CI III 2 pathway. The calculated TST high-pressure limit rate coefficients are summarized in Table 4. The free energy of activation of TS III2 pathway is lower, leading to 4-oxo-pentanal and CI III 2 which is 1.1 kcal more stable than propanone and CI III 1. For 6-hydroxy-POZ decomposition, the pathway leading to 4-oxo-pentanal and CI IV 1 has a free energy of activation 3.11 kcal mol^{-1} lower than that of the glycolaldehyde and CI IV 2 pathway. Because the primary ozonides are highly chemically activated, the further decomposition is very fast, and small differences, of a few kilocalories per mole in the activation barriers, will have a negligible impact on the branching ratio of the decomposition. Rate coefficients for these reactions should be calculated by using the microcanonical unimolecular rate equations and by considering the distribution of energies and the energy transfer processes.[20]

IV. Conclusions

This paper presents the first theoretical study of the reactions of ozone with geraniol-trans, 6-methyl-5-hepten-2-one, and 6-hydroxy-4-methyl-4-hexenal. These reactions are initiated by the formation of van der Waals complexes to yield primary ozonides, which rapidly open to carbonyl oxide compounds.

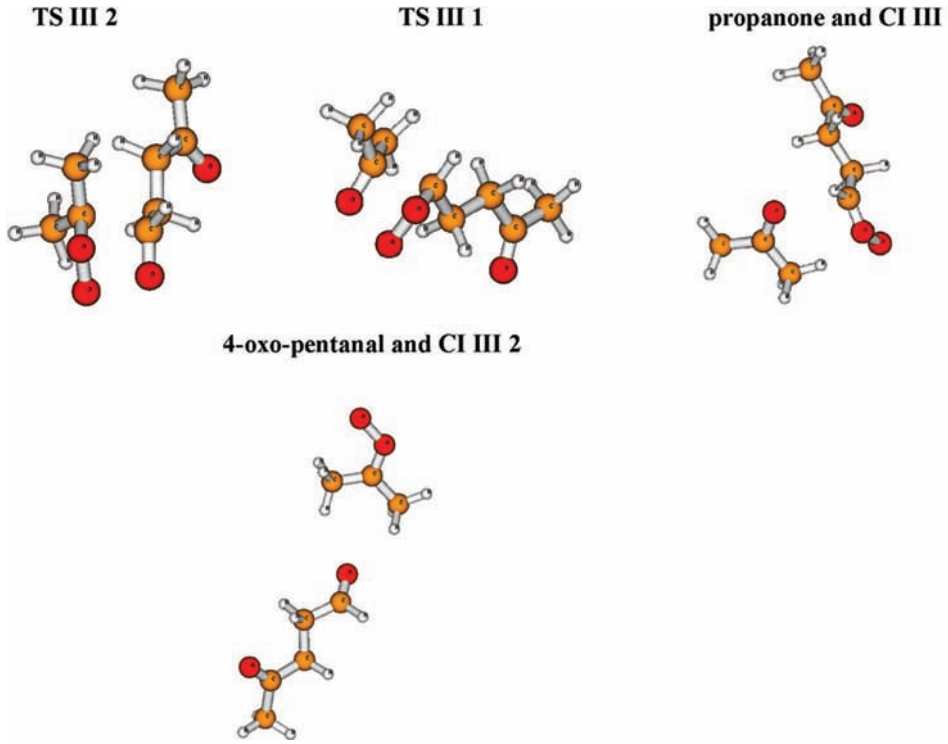

Figure 6. Optimized geometries of TS III 1, TS III 2, propanone, 4-oxo-pentanal, CI III 1, and CI III 2 associated with cleavage of the primary ozonide 6-methyl-POZ at the BH&HLYP/cc-pVDZ level of theory.

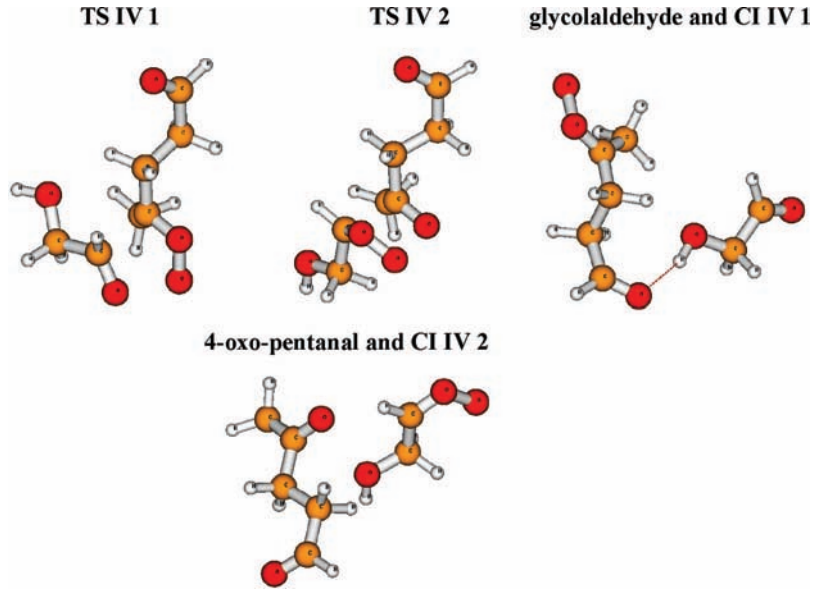

Figure 7. Optimized geometries of TS IV 1, TS IV 2, glycolaldehyde, 4-oxo-pentanal, CI IV 1, and CI IV 2 associated with cleavage of the primary ozonide 6-hydroxy-POZ at the BH&HLYP/cc-pVDZ level of theory.

The reaction barrier heights for the formation of POZs have first been determined. The reaction from reactants to POZ is predicted to be the rate-controlling step of the oxidation process. A combined quantum-chemical and TST approach has been employed to determine the structures and energies of relevant species in the reaction systems following the Criegee mechanism and to predict the kinetics and mechanism of geraniol-trans, 6-methyl-5-hepten-2-one, and 6-hydroxy-4-methyl-4-hexenal ozonolysis. The present results provide novel aspects for these reactions, which are valuable to interpret previous experimental results.

The addition reactions are highly exothermic, with the reaction energies of −71.80 and −73.97 kcal mol^{-1} for geraniol-trans, −71.20 kcal mol^{-1} for 6-methyl-5-hepten-2-one, and −73.72 kcal mol^{-1} for 6-hydroxy-4-methyl-4-hexenal at the BH&HLYP/cc-pVDZ level. The results obtained in this study are in agreement with the ranking proposed by Zhao and Truhlar,[13] who demonstrated that BH&HLYP functional showed a better performance in describing unbonded interactions than the other functionals. All these results indicate the importance of the fraction of Hartree−Fock exchange integrals, included in the exchange functional, for a better description of unbonded interactions.

According to the calculations, the 6-methyl-5-hepten-2-one reaction is faster than the 6-hydroxy-4-methyl-4-hexenal reac-

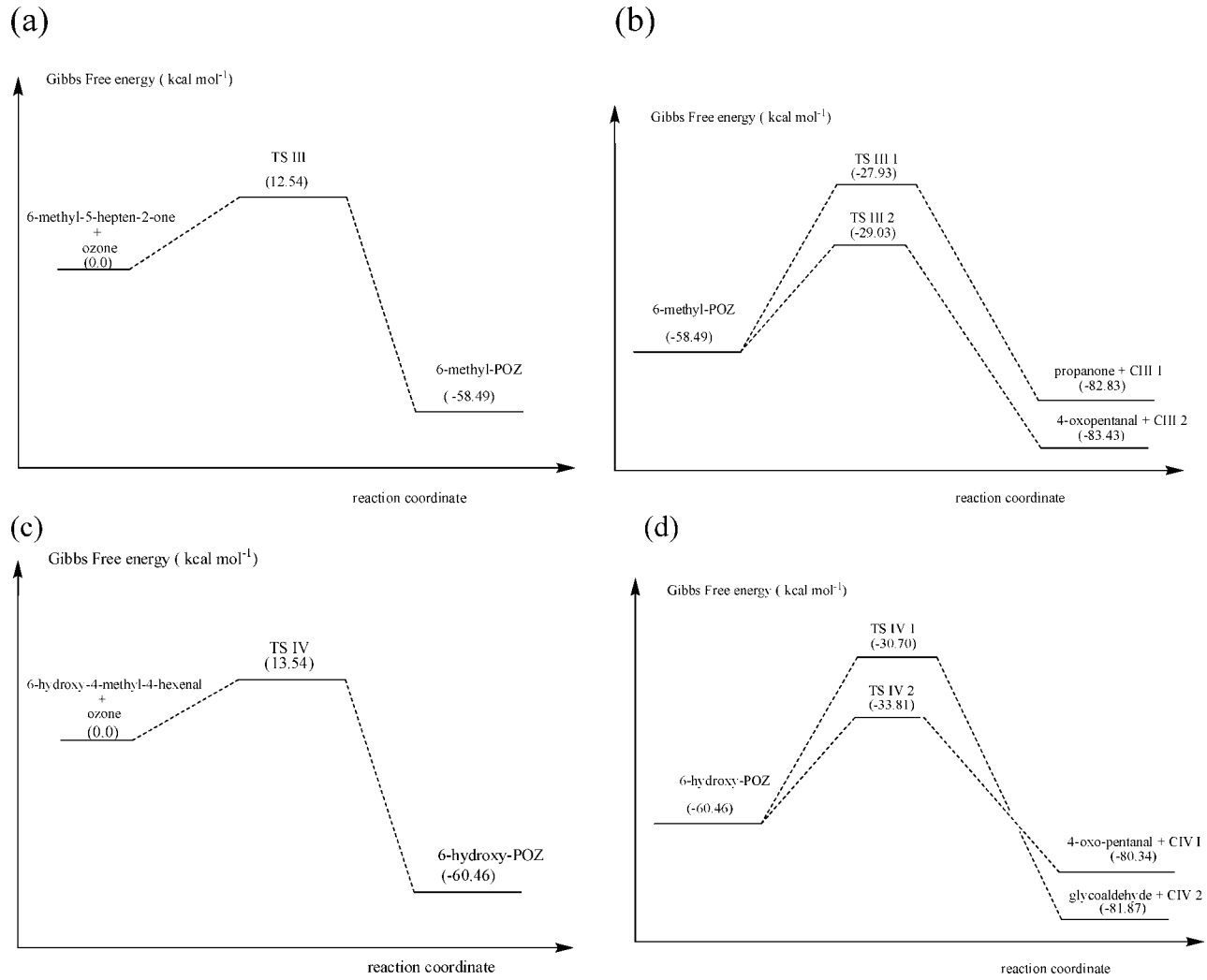

Figure 8. Gibbs free-energy profile for (a) 6-methyl-5-hepten-2-one and (c) 6-hydro-4-methyl-4-hexenal ozonolysis. (b and d) cleavage of primary ozonides.

TABLE 4: Calculated TST Rate Coefficients for the Intermediate Pathways of 6-Methyl-5-hepten-2-one and 6-Hydroxy-4-methyl-4-hexenal Ozonolysis Reactions at 298 K at the BH&HLYP/cc-pVDZ Level of Theory[a]

pathway	k
III	6.6×10^{-18}
III 1	4.0×10^{-31}
III 2	1.6×10^{-36}
IV	1.2×10^{-18}
IV 1	1.5×10^{-30}
IV 2	3.0×10^{-28}

[a] Units of s^{-1} and cm^3 $molecule^{-1}$ s^{-1} for unimolecular and bimolecular coefficients, respectively.

tion, but both are slower than the geraniol-trans reaction. For the geraniol-trans reaction, O_3 addition on site 1 is faster than on site 2.

It should be noted that the experimental rate coefficients as determined by Forester et al.[5] and Andrade et al.[10] were obtained by following the O_3 concentrations profile. Because in both studies, initial ozone concentrations were about 10 times higher than geraniol-trans concentrations, the reactions proceeded up to the consumption of the primary products, 6-methyl-5-hepten-2-one and 6-hydroxy-4-methyl-4-hexenal. Therefore, the experimental rate of O_3 consumption is a global value corresponding to the sum of pathways I, II, III, and IV. Because this rate is dominated by the first step and, to a minor extent, by the second step, which are at least one order of magnitude higher than paths III and IV, the apparent rate coefficient was estimated by adding the rate coefficients of pathways I and II (Table 4). It should be noted also that the uncertainties in the energy barriers are about 1 kcal mol^{-1}, which leads to an error of at least one order of magnitude in the rate coefficients. The calculated sum of 5.9×10^{-16} cm^3 $molecule^{-1}$ s^{-1} at the BH&HLYP/cc-pVDZ level of theory is in good agreement with the experimental studies Table 2.

Acknowledgment. The authors acknowledge additional support from the CNPq and CAPES.

Supporting Information Available: Tables of absolute energies, zero-point energies, and free energy for all the species investigated in this study are provided in the supporting materials. This material is available free of charge via the Internet at http://pubs.acs.org.

References and Notes

(1) Zimmerman, P. R.; Chatfield, R. B.; Fishman, J.; Crutzen, P. J.; Hanst, P. *Geophys. Res. Lett.* **1978**, *5*, 679–682.

(2) Guenther, A.; Hewitt, C. N.; Erickson, D.; Fall, R.; Geron, C.; Graedel, T.; Harley, P.; Klinger, L.; Lerdau, M.; McKay, W. A.; Pierce, T.; Scholes, B.; Steinbrecher, R.; Tallamraju, R.; Taylor, J.; Zimmerman, P. *Geophys. Res.* **1995**, *100*, 8873.

(3) Evans, W. C. *Trease and Evans' Pharmacognosy*; W.B. Saunders Company Ltd.: London, 1996; pp 255−293.

(4) (a) Craveiro, A. A.; Fernandes, A. G.; Andrade, C. H. S.; Matos, F. J. A.; Alencar, J. W.; Machado,M. I. L. *Óleos essenciais de plantas do Nordeste*; Edições UFC: Fortaleza1981; pp 20−170. (b) Nazaroff, W. W.; Weschler, C. J. *Atmos. Environ.* **2004**, *38*, 2841–2865.

(5) (a) Forester, C. D.; Ham, J. E.; Wells, J. R. *Atmos. Environ.* **2007**, *41*, 1188–1199. (b) Hoffmann, T.; Bandur, R.; Marggraf, U.; Linscheid, M. *J. Geophys. Res.* **1998**, *103*, 25569–25578. (c) Zhang, R.; Suh, I.; Zhao, J.; Zhang, D.; Fortner, E. C.; Tie, X.; Molina, L. T.; Molina, M. J. *Science* **2004**, *304*, 1487–1490.

(6) Zhang, D. R. *J.Chem. Phys. A* **2005**, *122*, 114308.

(7) Bailey, P. S. *Olefinic Compounds*; Academic Press: New York, 1978; Vol. I

(8) Griesbaum, K.; Miclaus, V.; Jung, I. C. *Environ. Sci. Technol.* **1998**, *32*, 647–649.

(9) Grosjean, E.; Grosjean, D.; Seinfeld, J. H. *Int. J. Chem. Kinet.* **1996b**, *28*, 373–382.

(10) Nunes, F. M. N.; Veloso, M. C. C.; Pereira, P. A. P.; Andrade, J. B. *Atmos. Environ.* **2005**, *39*, 7715–7730.

(11) Cremer, D.; Kraka, E.; Szalay, P. G. *Chem. Phys. Lett.* **1998**, 292,–97.

(12) Li, S. Q.; Yang, J.; Zhang, S. J. *Phys. Chem. A* **2005**, *109*, 9284–9291.

(13) Zhao, Y.; Truhlar, D. G. *J. Chem. Theory. Comput.* **2005**, *1*, 415–432.

(14) Frisch, M. J.; Trucks, G. W.; Schlegel, H. B.; Scuseria, G. E.; Robb, M. A.; Cheeseman, J. R.; Zakrzewski, V. G.; Montgomery, J. A., Jr.; Stratmann, R. E.; Burant, J. C.; Dapprich, S.; Millam, J. M.; Daniels, A. D.; Kudin, K. N.; Strain, M. C.; Farkas, O.; Tomasi, J.; Barone, V.; Cossi, M.; Cammi, R.; Mennucci, B.; Pomelli, C.; Adamo, C.; Clifford, S.; Ochterski, J.; Petersson, G. A.; Ayala, P. Y.; Cui, Q.; Morokuma, K.; Malick, D. K.; Rabuck, A. D.; Raghavachari, K.; Foresman, J. B.; Cioslowski, J.; Ortiz, J. V.; Stefanov, B. B.; Liu, G.; Liashenko, A.; Piskorz, P.; Komaromi, I.; Gomperts, R.; Martin, R. L.; Fox, D. J.; Keith, T.; Al-Laham, M. A.; Peng, C. Y.; Nanayakkara, A.; Gonzalez, C.; Challacombe, M.; Gill, P. M. W.; Johnson, B. G.; Chen, W.; Wong, M. W.; Andres, J. L.; Head-Gordon, M.; Replogle, E. S.; Pople, J. A. *Gaussian 98*, revision D.3; Gaussian, Inc.: Pittsburgh, PA, 1998.

(15) Lynch, B. J.; Fast, P. L.; Harris, M.; Truhlar, D. G. J. *Phys. Chem. A* **2000**, *104*, 4811.

(16) Adamo, C.; Barone, V. *J. Chem. Phys.* **1998**, *108*, 664.

(17) Li, Q. S.; Xu, X. D.; Zhang, S. *Chem. Phys. Lett.* **2004**, *384*, 20.

(18) Lynch, B. J.; Truhlar, D. G. *J. Phys. Chem. A* **2001**, *105*, 2936.

(19) Stephens, P. J.; Devlin, F. J.; Chabalowski, C. F.; Frisch, M. J. *J. Phys. Chem. A* **1994**, *98*, 11623.

(20) (a) Gilbert, R. G.; Smith, S. C. *Theory of unimolecular and recombination reactions*; Blackwell: Oxford, 1990. (b) Steinfeld, J. I.; Francisco, J. S.; Hase, W. L. *Chemical kinetics and dynamics*; Prentice Hall: Upper Saddle River, 1998.

(21) Cremer, D.; Pople, J. *J. Am. Chem. Soc.* **1975**, *97*, 1354.

JP8027534